

VIDEOLIGHTS: Feature Refinement and Cross-Task Alignment Transformer for Joint Video Highlight Detection and Moment Retrieval

Dhiman Paul^{*}, Md Rizwan Parvez^{*}, Nabeel Mohammed^{*} and Shafin Rahman^{*}

Abstract—Video Highlight Detection and Moment Retrieval (HD/MR) are essential in video analysis. Recent joint prediction transformer models often overlook their cross-task dynamics and video-text alignment and refinement. Moreover, most models typically use limited, uni-directional attention mechanisms, resulting in weakly integrated representations and suboptimal performance in capturing the interdependence between video and text modalities. Although large-language and vision-language models (LLM/LVLMs) have gained prominence across various domains, their application in this field remains relatively underexplored. Here we propose VideoLights, a novel HD/MR framework addressing these limitations through (i) Convolutional Projection and Feature Refinement modules with an alignment loss for better video-text feature alignment, (ii) Bi-Directional Cross-Modal Fusion network for strongly coupled query-aware clip representations, and (iii) Uni-directional joint-task feedback mechanism enhancing both tasks through correlation. In addition, (iv) we introduce hard positive/negative losses for adaptive error penalization and improved learning, and (v) leverage LVLMs like BLIP-2 for enhanced multimodal feature integration and intelligent pretraining using synthetic data generated from LVLMs. Comprehensive experiments on QVHighlights, TVSum, and Charades-STA benchmarks demonstrate state-of-the-art performance. Codes and models are available at: <https://github.com/dpaul06/VideoLights>.

Index Terms—video highlight detection, moment retrieval, video grounding, feature refinement,

I. INTRODUCTION

THE surge in digital devices, platforms, and internet usage has led to abundant online video content [1], [2]. However, navigating through such vast content poses an exceedingly difficult challenge for users, impeding their ability to pinpoint specific points of interest within recordings [1], [3]. Consequently, Video Highlight Detection (HD; [4]–[8]) and Moment Retrieval (MR; [3], [9]–[15]), which evaluate saliency scores of video clips and automatically identify significant moments (i.e. clips with the highest saliency scores) for user queries, respectively, have become indispensable tools in video analysis—streamlining content management, recommendation, creation, editing, and event detection processes. Given their

shared objective of ranking/localizing the relevant video clips based on user queries and the commonality in their multimodal models and data properties, recent studies using transfer models have begun to jointly model Video Highlight Detection and Moment Retrieval (HD/MR) [16]–[23].

Text and video feature embeddings derived from vision-language models (VLMs), such as CLIP [24] and BLIP [25], facilitate a nuanced and fundamental understanding of text and video modalities. By utilizing pre-trained embeddings, these models have shown significant effectiveness in tackling complex challenges related to semantic alignment and multimodal reasoning, thereby improving the integration and interpretability of multimodal data. For joint MR-HD tasks, most studies [16]–[22] primarily employ textual and visual features from CLIP pre-trained on Kinetics 400 [26]. However, since CLIP is mainly trained on static images and text, it lacks the temporal information critical for video understanding. To address this limitation, additional visual embeddings from SlowFast [27], which incorporate both visual and temporal aspects, are integrated [16]. While CLIP learns joint representations across text and images, Large Vision-Language Models (LVLMs) like GPT-4V [28], LLaVA [29], or BLIP-2 [30] have emerged as more powerful tools with complex reasoning capabilities and proven success across various tasks in vision and language domains [31]. Therefore, at the very root of our study for joint HD/MR prediction tasks, we introduce enhanced visual and textual embeddings augmented from all of CLIP, SlowFast and the LVLM BLIP-2 [30], which have been predominantly underexplored in HD/MR literature. We verify its effectiveness over existing embeddings such as CLIP (in Section IV-A and IV-B).

Nonetheless, joint HD/MR prediction is a challenging task requiring a deeper understanding of both text and video modalities, as well as their cross-modal and cross-task synergies. Despite their coexistence and correlations, we observe that most approaches undermine either the cross-task (i.e., HD vs. MR) or cross-modal (i.e., text vs. video) dynamics when modeling them jointly, thereby limiting potential gains and robustness. For example, the early work Moment-DETR [16], based on an encoder-decoder transformer model, employs the concatenation of pre-trained vision-language model features for video and text representation. Follow-up works like UMT [17] augment audio inputs in the encoder and text in the decoder while using isolated text and video features. QD-DETR [19] develops a query-dependent video representation module that aligns text with video. UniVTG [20] further presents a multi-

Manuscript received December 1, 2024. (Corresponding author: Shafin Rahman)

Dhiman Paul, Nabeel Mohammed, and Shafin Rahman are with the Department of Electrical and Computer Engineering, North South University, Dhaka, Bangladesh (email: dhiman.paul@northsouth.edu; nabeel.mohammed@northsouth.edu; shafin.rahman@northsouth.edu).

Md Rizwan Parvez is with Qatar Computing Research Institute (QCRI), Qatar (email: mparvez@hbku.edu.qa).

* Equal contribution.

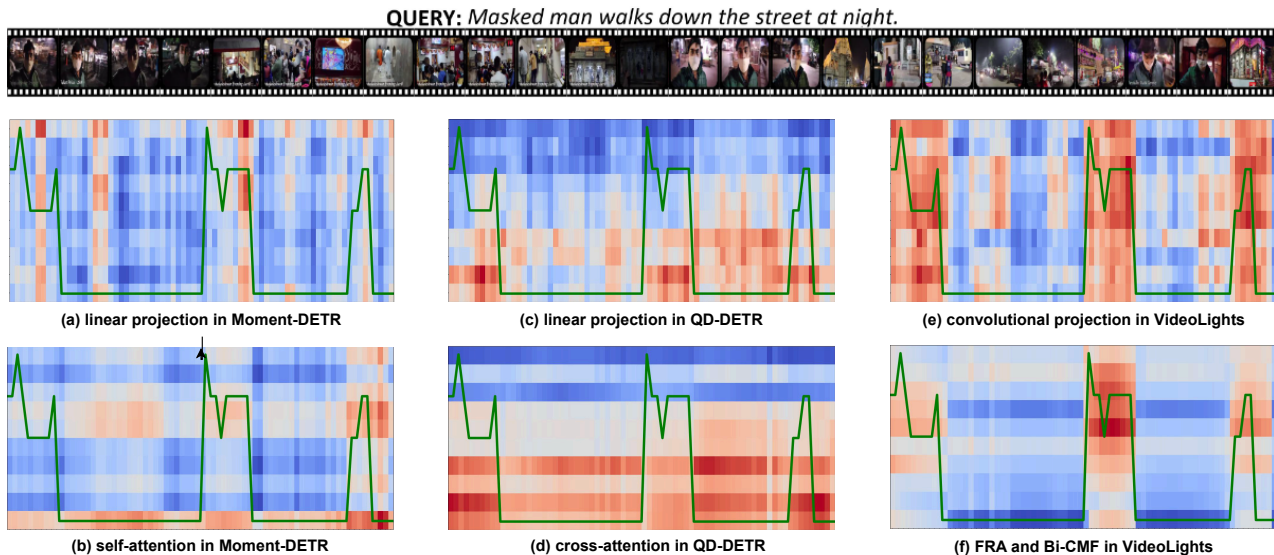


Fig. 1. Relevance heat map illustrating multimodal alignment dynamics across video understanding models. Color intensity (blue to red) quantifies query-video clip correspondence, with the green line indicating ground truth clip-wise saliency. Comparative visualization reveals **VideoLights**'s progressive refinement of query-clip relevance through projection, feature refinement, and bi-directional cross-attention stages, in contrast to Moment-DETR [16] and QD-DETR [19]'s limited multimodal interaction.

task learning approach using unified finetuning and pretraining methods. These methods cascade two isolated task heads after the shared layers without addressing cross-task interactions. On the other hand, the recently proposed TaskWeave [18] and TR-DETR [22] models address (bi-directional) cross-task relations by first computing HD and MR independently, then having them cooperate (HD into MR and vice versa) to recompute the results, but they still rely on no or unidirectional (cross-modal) attention from text to video, respectively. To address these challenges, in this paper, we propose a new HD / MR joint prediction framework **VideoLights** that enables learning from cross-modal and cross-task interactions. Moreover, in many instances, text queries tend to be more concise, whereas video frames often contain noisy and irrelevant information. Consequently, directly applying attention to the entire video does not effectively differentiate between relevant and irrelevant clips. TR-DETR addresses this challenge by enhancing visual tokens in relation to query tokens. To tackle this issue, we have developed a Feature Refinement and Alignment (FRA) Module, which adeptly refines visual features in accordance with textual features and aligns them at local and global levels. Fig. 1 visually shows that only self-attention or cross-attention cannot effectively align the query-video.

At the core of our framework are the following modules and principles:

- 1) **Feature Refinement and Alignment (FRA) Module:** Implements CNN-based intramodal and intermodal feature interaction and refinement, with intermodal alignment loss for text-video correspondence.
- 2) **Bi-Directional Cross-Modal Fusion (Bi-CMF) Network:** Employs a multi-stage hierarchical process for bidirectional text-video attention, yielding a strongly coupled query-aware clip representation.

- 3) **Unidirectional Joint-Task Feedback Mechanism (Uni-JFM):** Enhances task correlation through task-specific and task-coupled losses, utilizing cosine similarity on feature vectors from HD and MR, improving cross-task learning efficiency.
- 4) **Adaptive Error Correction:** Incorporates hard positive and hard negative losses to adaptively penalize model errors in clip saliency prediction, fostering improved learning.
- 5) **Intelligent Model Pre-training:** Capitalizing on the image-to-text generation capabilities in Large Vision-Language Models (LVLMs), specifically BLIP-2, utilizes synthetic data generated from video corpora and language-image models to create high-quality paired text queries for model pre-training.

We perform comprehensive evaluations on widely recognized benchmarks QVHighlights [16], TVSum [32], and Charades-STA [9]. Results show that in both tasks, **VideoLights** achieves strong performance, outperforming all previous baselines by a significant margin (an average of 1.4% in QVHighlights, 0.7% in TVSum, and 0.3% in Charades-STA) and achieving their new state-of-the-art results. We also provide an in-depth ablation study of our model on the QVHighlights development set, visualize the qualitative examples, and analyze the effects of different synthetic pre-training corpus and the impact of feature ensembles. We will open-source our implementation accordingly.

II. RELATED WORK

Moment retrieval (MR) and highlight detection (HD) are closely related tasks in video understanding. MR aims to retrieve video moments relevant to a given natural language query, while HD focuses on detecting the most important or

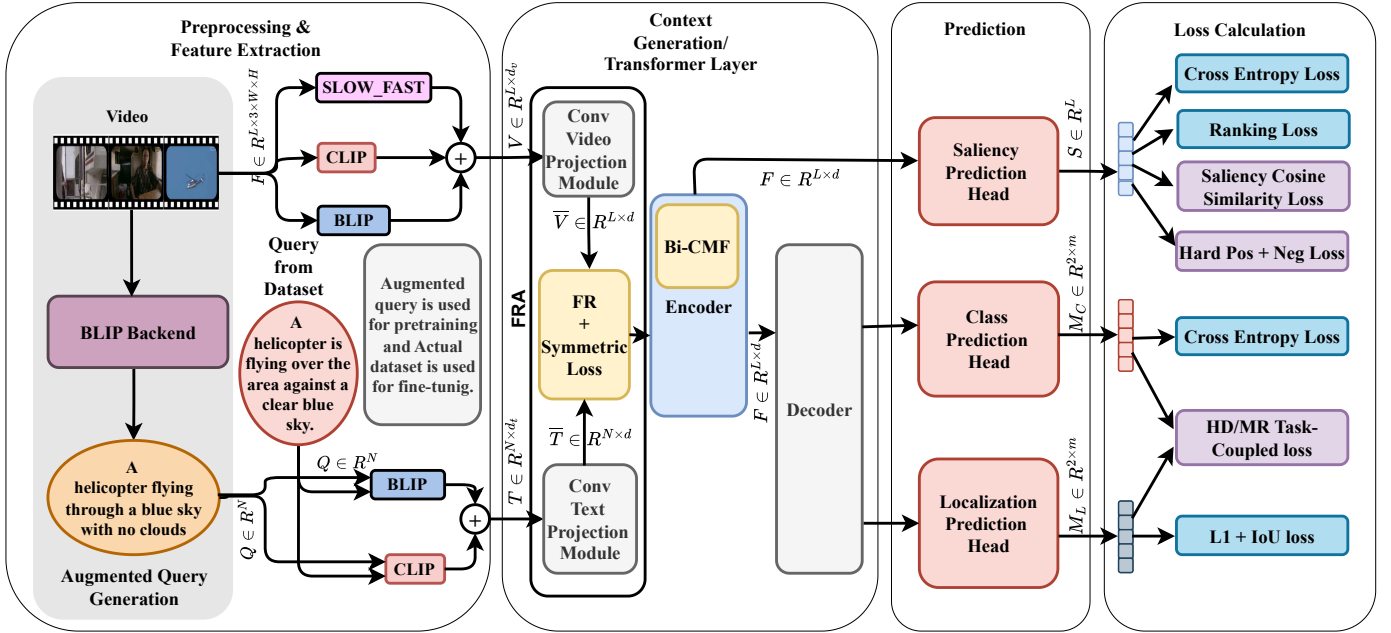


Fig. 2. Overall **VideoLights** architecture. FRA models the video-text cross-modal correlations from projected embeddings and passes them to Bi-CMF in the encoder. A trainable saliency vector predicts output saliency levels. Class and moment prediction heads predict logits and video moments, while saliency cosine similarity and task-coupled HD/MR losses together provide cross-task feedback *Uni-JFM*. Proposed new losses are in purple.

salient moments in a video. Early MR approaches include two-stage methods [3], [9], [33]–[36] and one-stage methods [35], [37]–[51]. But recent research on MR and HD has primarily advanced transformer-based architectures [52]. The detection transformer model (DETR) [53] leverages vision transformers to simplify predictions by eliminating the need for anchor generation and non-maximum suppression. Despite initial convergence delays, subsequent advances have made DETR widely applied in HD and MR. A standout contribution is Moment-DETR [16], which introduced the QVHighlights dataset for concurrent HD/MR. Moment-DETR is a modified iteration of the DETR model, excelling at pinpointing query-relevant moments and their corresponding saliency scores. Another recent work, UMT [17], proposed a unified architecture for processing multimodal data (video and audio) for MR and HD. However, UMT removes the moment decoder and bipartite matching from Moment-DETR, resulting in inferior MR performance. Additionally, some works have explored alternative approaches to MR and HD. For example, TVT [54] utilized additional data (subtitles) to capture relevant moments, while FVMR [55] improved inference speed for efficient MR. A novel Reversed Recurrent Tuning (R²-Tuning) [56] framework leverages CLIP’s multi-layer features for efficient, parameter-light video temporal grounding across diverse tasks and benchmarks. As MR and HD tasks are relevant to each other, some recent methods (TaskWeave [18], TR-DETR [22]) explored the cross-task dependence effectively. However, in this paper, we develop a joint prediction HD/MR model focusing on cross-modal and cross-task interplays. We open

Cross-modal learning relies on integrating and synchronizing information from different modalities, such as visual images and textual data. Several models, such as TERAN [57], HGSPN [58], and AVS [59], [60] have explored this topic. Unloc [61], a recent effort, uses a cross-modal fusion of

CLIP [24] text and video tokens to create a feature pyramid employing CNN prediction layers for Moment Retrieval, Temporal Localization, and Action Segmentation in a single-stage model. However, they are mainly limited to different text-to-video attention. Differently, we have used a custom cross-modal fusion module to find the bi-directional interrelation between text query and video clips and leverage this in the decoder with additional cross-task supervision.

Several recent studies have explored the use of weakly supervised pretraining approaches with data from various modalities, demonstrating improvements in model performance [16], [17], [20], [61], [62]. Some of them have utilized Automatic Speech Recognition (ASR) captions as query text to [16], [17], [62]. Similarly to us, [61] have employed a pre-training strategy that involves initially training their CLIP backend with the Kinetics-700 dataset [63] before fine-tuning the model for downstream tasks. UniVTG [20], on the contrary, collected a large training corpus combining the Ego4D dataset [64] and VideoCC [65] while ours shows more robustness without such data diversity. In text-only context, [66] shows that combining different encoders can facilitate enhanced supervision.

III. PROPOSED **VideoLights** MODEL

We present **VideoLights**, our joint prediction HD/MR model that enables learning from cross-modal (text vs video) and cross-task (HD vs MR) interplays. **VideoLights** features a unique composite of a Bi-Directional Cross-Modal Fusion Network, a Unidirectional Join-Task Feedback module, advanced appetite loss functions, and intelligent model training. **VideoLights** pipeline is depicted in Fig. 2.

A. Model Overview

Highlight Detection (HD) and Moment Retrieval (MR) aim to estimate the saliency of video clips and identify significant

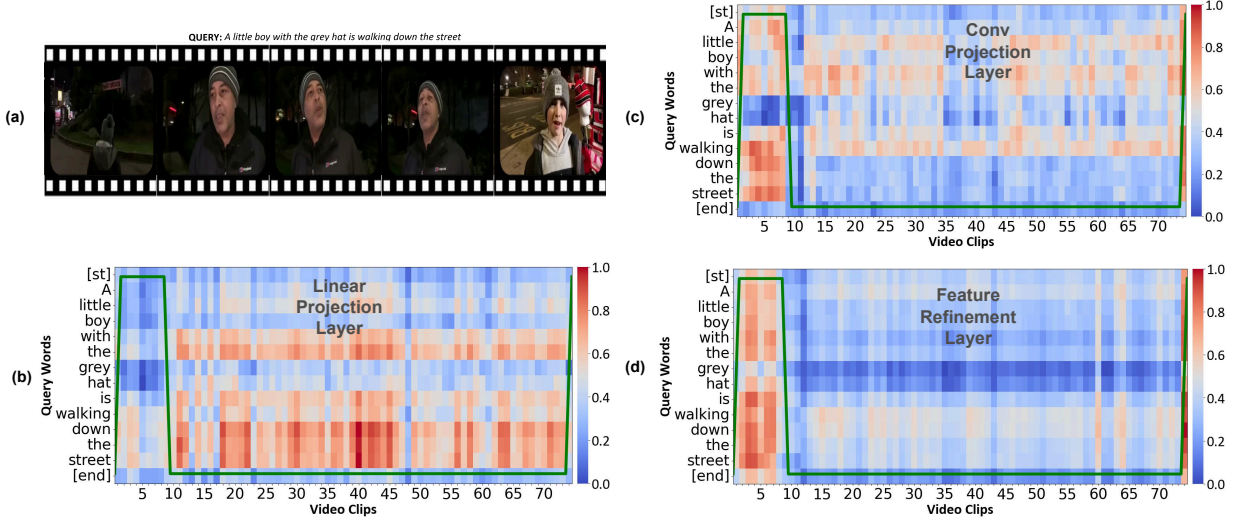


Fig. 3. (a) is the input video, (b) and (c) are correspondence maps of query and video tokens using linear and convolution layers, respectively, which show that queries are more aligned for the convolution layer, video, and text than linear projection layers. (d) The effect of the Feature Refinement module that effectively aligns video and text tokens that match ground truth saliency levels (green line) in each heat map saliency level is shown with green line plot.

moments for a given text query. Given a video of L clips, we define the video clips as $F \in \mathbb{R}^{L \times 3 \times W \times H}$, where W and H denote the width and height of the video, and 3 represents the number of color channels. The feature representation of the video is denoted as $V \in \mathbb{R}^{L \times d_v}$, where d_v is the feature dimension extracted by a frozen video encoder. Given a text query of N tokens, the representation of the text is denoted as $T \in \mathbb{R}^{N \times d_t}$, where d_t is the feature dimension extracted by a frozen text encoder. With these representations and given the video and the text, our goal is twofold: for Moment Retrieval (MR), we aim to determine all the moments $M \in \mathbb{R}^{2 \times m}$, where each moment consists of a central coordinate m_c and width m_σ , identifying m such moments within the video. For Highlight Detection (HD), we aim to rank the saliency scores $S \in \mathbb{R}^L$ for each clip in the video to detect highlights.

Embeddings: We compute the initial feature sets V and T from multiple different VLPs as follows:

$$T = \text{clip}(Q) \oplus \text{blip}(Q)$$

$$V = \text{clip}(F) \oplus \text{slowfast}(F) \oplus \text{blip}(F)$$

Here \oplus operator denotes concatenation of the features and clip, blip, and slowfast refer to frozen CLIP [24], BLIP-2 [30], and Slow-Fast models [27] respectively.

Projection and Alignment: When combining V and T for further processing, their differing hidden dimensions can make merging challenging. We address this issue by aligning the feature dimensionalities of the video and text representations using a Feed Forward Network (FFCNN) consisting of convolution layers. After this step, $V \in \mathbb{R}^{L \times d_v}$ becomes $\bar{V} \in \mathbb{R}^{L \times d}$ and $T \in \mathbb{R}^{N \times d_t}$ becomes $\bar{T} \in \mathbb{R}^{N \times d}$, where d is the dimension of the hidden layer.

$$\bar{V} = \text{relu}(\text{FFCNN}(V)), \quad \bar{T} = \text{relu}(\text{FFCNN}(T))$$

After this, Both video and text representations are passed to the video-query refinement module to learn query-attended video

representations and highlight relevant video tokens. Details are discussed in Section III-B.

Encoder with Cross-Modal Interaction Refined video tokens and query tokens are sent to our cross-modal interaction module *Bi-CMF* (discussed in Section III-C). This module fuses video and text features to learn their inter-relevance and learns a strongly coupled query-injected video representation. Then, in the multilayer encoder, self-attention is applied to the output of the Bi-CMF. Then, the output is then used to predict the saliency level of each clip.

Decoder with Cross-Task Dynamics Furthermore, the fused representation is sent to a decoder module following the work [19]. The output of this module is used in the class prediction head and the localization prediction head to predict the foreground-background class and moments in the video. Negative relations between irrelevant video-text queries are used to fine-tune the response, similar to what was done in [19]. We propose a new learning module, the unidirectional cross-task feedback network *Uni-JFM*. *Uni-JFM* takes one task HD as a reference and computes its additional losses: a task-specific (from HD) and a cross-task (from MR) losses discussed in Section III-E.

Adaptive Learning and Loss Functions *VideoLights* utilizes different losses for moment retrieval and highlight identification. We utilize L1, gIoU [67] $\mathcal{L}_{gIoU}(m, \bar{m})$, and cross-entropy \mathcal{L}_{cls} objectives to perform moment retrieval like [16]. Additionally, we have used margin ranking loss \mathcal{L}_{rank} , rank contrastive loss \mathcal{L}_{cont} like [19], and entropy loss for highlight identification. Then total loss is the summation of highlight loss and moment loss. For alignment, from FRA, we used symmetric alignment loss \mathcal{L}_{sym} . For saliency prediction (i.e., in HD), we have introduced two adaptive hard negative loss $\mathcal{L}_{hard_{neg}}$, hard positive loss $\mathcal{L}_{hard_{pos}}$ (discussed in Section III-D). These losses penalize errors in saliency prediction that persist with iterations.

In summary, the formulation of moment loss \mathcal{L}_{mr} can be

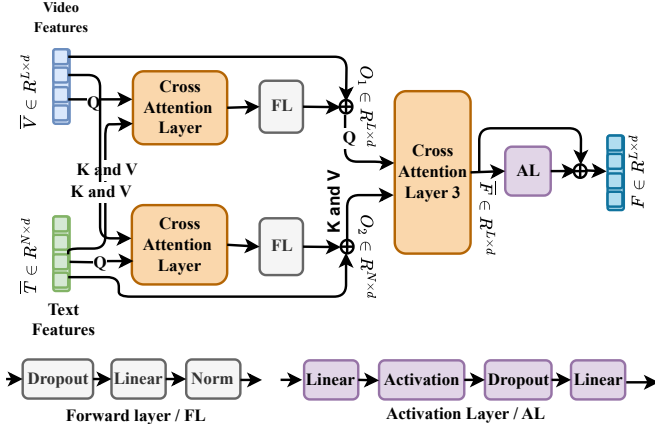


Fig. 4. Bi-CMF learns query-oriented video via text2video, video2text, then text2video attentions. In this process, dropout and normalization are applied after each step, and activation is applied at the last stage.

expressed as follows:

$$\mathcal{L}_{mr} = \lambda_{L1} \|m - \bar{m}\| + \lambda_{gIoU} \mathcal{L}_{gIoU}(m, \bar{m}) + \lambda_{cls} \mathcal{L}_{cls} \quad (1)$$

As the additional $\mathcal{L}_{hard_{neg}}$, $\mathcal{L}_{hard_{pos}}$ as well as $\mathcal{L}_{Uni-JFM}$ losses are computed in saliency prediction, we denote the overall saliency loss as follows:

$$\begin{aligned} \mathcal{L}_{hl} = & \lambda_{rank} \mathcal{L}_{rank} + \lambda_{cont} \mathcal{L}_{cont} \\ & + \mathcal{L}_{hard_{neg}} + \mathcal{L}_{hard_{pos}} + \mathcal{L}_{Uni-JFM} \end{aligned} \quad (2)$$

Additionally, for assisting FRA, we have introduced alignment loss \mathcal{L}_{align} discussed in Section III-B. Therefore, the final total loss is:

$$\mathcal{L}_{total} = \lambda_{sal} \mathcal{L}_{hl} + \mathcal{L}_{mr} + \lambda_{al} \mathcal{L}_{align} \quad (3)$$

where the hyperparameters λ_{sal} , λ_{al} are used to achieve a balance between these losses. In the following we discuss the *Bi-CMF* and *Uni-JFM* modules, Adaptive $\mathcal{L}_{hard_{neg}}$, $\mathcal{L}_{hard_{pos}}$ losses, and our pretraining procedure.

B. Feature Refinement and Alignment Network: FRA

Text queries are typically concise and informative, whereas video clips often contain substantial noise and irrelevant information. When self-attention or cross-attention mechanisms are applied directly to video tokens, all tokens are weighted equally, which can result in insufficient emphasis on the truly relevant tokens. To address this limitation, we propose the Feature Refinement and Alignment Network (FRA). FRA facilitates both local (clip or word level) and global (video or sentence level) alignment between video and query tokens through a two-stage process.

In the first stage, a convolutional projection layer captures local representations, aligning video and text features while also adjusting token dimensions. In the second stage, the feature refinement layer promotes global alignment by computing an adjusted correspondence map, extracting sentence-level features, generating a similarity matrix, and aggregating the results. This refinement process highlights video tokens

that are semantically aligned with both sentence-level and word-level features.

Figure 3 illustrates the differences between standard linear projection and convolutional projection and refinement network, highlighting the enhanced focus on relevant video tokens, which results in improved similarity scores that align with the ground truth saliency score.

This refinement process is represented as:

$$\begin{aligned} V_Q &= \bar{V} \cdot \bar{T}^T, & S &= \text{pool}(\bar{T}), \\ V_S &= \bar{V} \cdot S^T, & S_v &= S \cdot \mathbf{1}_{1 \times V \times 1}, \\ V &= \text{conv}(\bar{V} \oplus V_Q \oplus V_S \oplus S_v) \end{aligned}$$

where \cdot means matrix multiplication.

To ensure alignment at the query-text level, we calculate the contrastive alignment loss between query tokens and projected query spans following [16]. This loss encourages higher similarity scores between the projected query spans and their corresponding text embeddings. It is defined as:

$$\begin{aligned} \mathcal{L}_{qt_align} = & \frac{1}{B} \sum_{b=1}^B \left(- \frac{\sum_m \text{logits}_{bm} \cdot \mathbb{1}_{\text{pos}}}{\text{num_pos}_b} \right. \\ & \left. + \log \sum_m \exp(\text{logits}_{bm}) \right) \end{aligned} \quad (4)$$

where $\text{logits}_{bm} = \frac{\sum_n (\mathbf{q}_{bm} \cdot \mathbf{t}_{bn})}{\tau}$, $\mathbb{1}_{\text{pos}}$ is an indicator for positive matches, and τ is the temperature and B is batch size.

To align video clips with corresponding sentence-level text embeddings, we calculate the video-text alignment loss by minimizing the cosine similarity error between their saliency scores.

$$\hat{s}_b = \frac{\bar{\mathbf{t}} \cdot \mathbf{v}}{\|\bar{\mathbf{t}}\| \|\mathbf{v}\|} \quad (5)$$

where $\bar{\mathbf{t}} = \frac{1}{N} \sum_{t=1}^N \mathbf{t}_t$. Here $\bar{\mathbf{t}}$ is the pooled sentence-level text embedding, \mathbf{v} is the clip-level video embedding, and \hat{s}_b is the calculated similarity score.

$$\mathcal{L}_{vt_align} = \frac{1}{B} \sum_{b=1}^B \left(1 - \frac{\text{norm}(\mathbf{s}_b) \cdot \text{norm}(\hat{\mathbf{s}}_b)}{\|\text{norm}(\mathbf{s}_b)\| \|\text{norm}(\hat{\mathbf{s}}_b)\|} \right) \quad (6)$$

where \mathbf{s}_b is the ground truth saliency score. The total loss is defined as:

$$\mathcal{L}_{align} = \mathcal{L}_{qt_align} + \mathcal{L}_{vt_align} \quad (7)$$

C. Bi-Directional Cross-Modal Fusion Network: Bi-CMF

To learn a strongly coupled, query-oriented video representation, we introduce our Bi-Directional Cross-Modal Fusion Network, *Bi-CMF*. It features three multi-head attention layers for cross-attention. Initially, a cross-attention layer uses projected video features as queries, while text data with positional embedding serve as keys and values, identifying video tokens conditioned by textual tokens. Similarly, another cross-attention layer is utilized to discern projected textual

tokens (query) features conditioned by video tokens fused with positional embedding (keys and values), enabling the identification of textual features pertinent to the video.

Subsequently, conditioned video tokens are used as queries, while conditioned textual tokens serve as keys and values in the final cross-attention layer, yielding fused contextual information that emphasizes video tokens relevant to the query. Further refinement is achieved through a self-attention mechanism applied to this fused context, allowing for the extraction of a more nuanced video context.

$$V_T = \text{attn}(\bar{V}, \bar{T}, \bar{T}), \quad T_V = \text{attn}(\bar{T}, \bar{V}, \bar{V}), \\ V_{\text{attn}} = \text{attn}(\bar{V}_T, \bar{T}_V, \bar{T}_V)$$

Residual connections [68], layer normalization [69], and dropout [70] mechanisms are implemented at each stage to enhance the robustness of the model, and encodings of learnable positions are incorporated into the input of each attention layer. *Bi-CMF* is depicted in Fig. 4.

D. Adaptive Loss Functions

We aim to enhance learning by identifying and rectifying persistent model errors. To achieve this, we design novel adaptive loss functions, specifically targeting hard positives and hard negatives. For the hard negative loss, we minimize the number of predictions in the negative regions where there are no relevant clips. Given the saliency score \bar{S}_i and the ground truth saliency score \mathcal{S}_i for non-relevant clips $i \in V_{neg}$, we define the loss,

$$\mathcal{L}_{hard_{neg}} = W_j \sum_{i \in V_{neg}} \text{abs}(\mathcal{S}_i - \bar{S}_i) \quad (8)$$

where W_j is a function of the j th epoch that penalizes more with a higher number of epochs. As in general, \mathcal{S}_i for $i \in V_{neg}$ is zero, the loss can be defined as:

$$\mathcal{L}_{hard_{neg}} = W_j \sum_{i \in V_{neg}} \text{abs}(\bar{S}_i) \quad (9)$$

For hard positive cases, we use Mean Square Error, and similarly, we define the loss as:

$$\mathcal{L}_{hard_{pos}} = W_j \sum_{i \in V_{pos}} \text{MSE}(\mathcal{S}_i, \bar{S}_i) \quad (10)$$

E. Unidirection Joint-Task Feedback Module (Uni-JFM)

To leverage the cross-task synergies while jointly predicting HD/MR, we devise a unidirectional joint-task feedback mechanism that is a composite of a task-specific and a task-coupled loss. We take HD as a reference task and compute its task-specific loss \mathcal{L}_{ts} . To do so, we calculate the saliency cosine similarity loss from the predicted saliency level. Here for saliency score \bar{S} and ground truth saliency score \mathcal{S} the saliency cosine similarity loss \mathcal{L}_{ts} can be defined as:

$$\mathcal{L}_{ts} = 1 - \frac{\bar{S} \cdot \mathcal{S}}{\|\bar{S}\| \|\mathcal{S}\|} \quad (11)$$

Next, for the task-coupled loss \mathcal{L}_{tc} , first, we use the feature vectors for MR, M to calculate saliency scores \bar{S}_{mr} following the MR2HD technique of [22] using a GRU unit. Then, differently, we calculate the similarity between the ground truth

Algorithm 1 Synthetic Data Generation Process

Require: Input video \mathcal{V} with duration T

Ensure: Synthetic dataset $\mathcal{D}_{\text{synthetic}}$

- 1: Divide the video \mathcal{V} into $n = \lceil T/10 \rceil$ non-overlapping intervals $\{I_1, I_2, \dots, I_n\}$, where each interval I_i corresponds to a 10-second segment of \mathcal{V} .
 - 2: **for** each interval I_i **do**
 - 3: Select a representative frame f_i from I_i (e.g., the middle frame or one sampled by a heuristic).
 - 4: Use the BLIP-2 model $\mathcal{M}_{\text{BLIP}}$ to generate a caption $c_i = \mathcal{M}_{\text{BLIP}}(f_i)$ describing the content of f_i .
 - 5: **end for**
 - 6: **for** each interval I_i **do**
 - 7: **for** each frame $f_{ij} \in I_i$ **do**
 - 8: Compute the cosine similarity $\text{Sim}(c_i, f_{ij})$ between the caption c_i and the frame f_{ij} using their feature representations $\phi(c_i)$ and $\phi(f_{ij})$.
 - 9: **end for**
 - 10: Use $s_i = \text{Sim}(c_i, f_{ij})$ for each video frame f_{ij} as frame-wise highlight scores for interval I_i .
 - 11: **end for**
 - 12: Construct a synthetic dataset $\mathcal{D}_{\text{synthetic}} = \{(c_i, I_i, s_i) \mid i \in [1, n]\}$, where c_i is the generated caption I_i is the corresponding interval and s_i is the saliency score.
 - 13: Use $\mathcal{D}_{\text{synthetic}}$ to train the target model for highlight detection or related tasks.
-

saliency \mathcal{S} and this calculated saliency \bar{S}_{mr} . This similarity score is used as the loss function \mathcal{L}_{tc} , where

$$\mathcal{L}_{tc} = 1 - \frac{\bar{S}_{mr} \cdot \mathcal{S}}{\|\bar{S}_{mr}\| \|\mathcal{S}\|} \quad (12)$$

The corresponding total loss for the module becomes,

$$\mathcal{L}_{Uni-JFM} = \mathcal{L}_{ts} + \mathcal{L}_{tc} \quad (13)$$

F. Pretraining

We propose a novel multi-step methodology to enhance attention-based networks' performance by addressing limitations in ASR caption-based weakly supervised training [16], [62]. ASR may not always align with or describe the content of the video of that timeframe. Our approach segments videos into 10-second intervals, generates descriptive captions using the BLIP model for representative frames, and creates synthetic data pairs from QVHighlights and Charades-STA datasets. Saliency scores are calculated based on frame-query similarity, and the resulting caption-query pairs are used for model training. While this process may generate noisy pretrain data, the subsequent finetuning helps filter out irrelevant information, leading to improved generalization [71]. Detailed data statistics and steps are provided in Table I and Algorithm 1.

IV. EXPERIMENTS

Datasets: We evaluate **VideoLights** using three widely recognized benchmarks to ensure a comprehensive and rigorous assessment. First, the *QVHighlights* dataset [16] uniquely

TABLE I
COMPARISON OF DATASETS USED IN THIS STUDY.

Dataset	Domain	Annotations	Videos	Task	Used in pt	Synthetic data
QVHighlights	Vlog / News	10.3K	12.5K	MR, HD	✓	187682
Charades-STA	Activity	16.1K	6.7K	MR	✓	23193
TVSum	Web	50	50	HD		

TABLE II
RESULTS ON QVHIGHLIGHTS TEST SPLIT. † REPRESENTS THE USE OF AUDIO MODALITY. HERE, BOLD REPRESENTS THE BEST RESULT, AND UNDERLINE REPRESENTS THE 2ND BEST RESULT.

Method	MR				HD		
	R1		mAP		Avg	>=Very mAP	Good HIT@1
	@0.5	@0.7	@0.5	@0.75			
Moment-DETR [16]	52.89	33.02	54.82	29.4	30.73	35.69	55.6
UMT [17] †	56.23	41.18	53.83	37.01	36.12	38.18	59.99
MH-DETR [72]	60.05	42.48	60.75	38.13	38.38	38.22	60.51
EaTR [21]	61.36	45.79	61.86	41.91	41.74	37.15	58.65
QD-DETR [19]	62.40	44.98	63.17	42.05	41.44	39.13	63.1
UVCOM [62]	<u>63.55</u>	47.47	63.37	42.67	<u>43.18</u>	39.74	<u>64.20</u>
TR-DETR [22]	64.66	48.96	63.98	43.73	42.62	<u>39.91</u>	63.42
UniVTG [20]	58.86	40.86	57.60	35.59	35.47	38.20	60.96
VideoLights	63.36	<u>48.70</u>	<u>63.81</u>	<u>42.87</u>	43.38	40.57	65.30
Moment-DETR(pt) [16]	59.78	40.33	60.51	35.36	36.14	37.43	60.17
UMT(pt) [17]	60.83	43.26	57.33	39.12	38.08	39.12	62.39
QD-DETR (pt) [19]	64.10	46.10	64.30	40.50	40.62	38.52	62.27
UVCOM(pt) [62]	64.53	48.31	<u>64.78</u>	43.65	<u>43.80</u>	39.98	65.58
UniVTG(pt) [20]	<u>65.43</u>	<u>50.06</u>	64.06	<u>45.02</u>	43.63	40.54	66.28
VideoLights-pt	68.48	52.53	67.31	46.76	45.01	41.48	65.89
VideoLights-B	68.29	52.79	67.58	47.30	46.53	42.43	68.94
VideoLights-B-pt	70.36	55.25	69.53	49.17	47.94	42.84	70.56

combines Moment and Highlight Detection tasks, providing extensive video annotations and maintaining evaluation impartiality through its online server. This dataset includes 12,562 YouTube videos and 10,310 annotations, with standardized data splits as per established works. Additionally, we use the *Charades-STA* [9] dataset for Moment Retrieval (MR) and the *TVSum* [32] dataset for Highlight Detection (HD). *TVSum*, encompasses ten categories with five videos each. We follow the data splits in [17], [19], [72], that consider 80% of the dataset for training and 20% for testing. *Charades-STA*, features 9,848 videos and 16,128 query texts, We adopt the data splits in prior work QD-DETR [19] with 12,408 samples for training and 3,720 for testing. Our adherence to these standardized splits and the diversity of datasets underscore our commitment to a robust and fair evaluation of **VideoLights**.

Evaluation Metrics: We follow the established evaluation metric standards from [16], [17], [19], [21], [72]. For moment retrieval, we calculate Recall@1 with predetermined thresholds of 0.5 and 0.7, mean average precision (mAP) with Intersection over Union (IoU) thresholds of 0.5 and 0.75, and average mAP across multiple IoU thresholds that range from 0.50 to 0.95. The same standards are applied to the QVHighlights dataset. For highlight identification, our evaluations include measuring mAP and HIT@1, indicating the hit ratio for the clip with the highest score.

Implementation details: We trained four models on each dataset: **VideoLights** and **VideoLights-pt**, which utilize CLIP and SlowFast features, and **VideoLights-B** and

VideoLights-B-pt, which incorporate CLIP, BLIP, and SlowFast features. For *TVSum*, we followed previous works such as TR-DETR [22] and used *I3D* [73], pre-trained on Kinetics 400 [26], to extract visual features in a variant of **VideoLights** for comparison with other methods. The models were configured with a hidden unit size of $d = 256$, one Bi-CMF layers (see Fig. 7), three encoder layers, three decoder layers, a seed value of 2018, and 10-moment queries. A dropout rate of 0.1 was applied to the transformer layers, and 0.5 to the input projection layers [16]. The loss hyperparameters were set as $\lambda_{L1} = 10$, $\lambda_{gIoU} = 1$, $\lambda_{cls} = 4$, $\lambda_{sal} = 1$, $\lambda_{rank} = 1$, $\lambda_{cont} = 1$, and $\Delta = 0.2$. Model weights were initialized using the Xavier initialization [74], and the model parameters were optimized with AdamW [75] using an initial learning rate of $1e-4$ and a weight decay of $1e-4$. Following [16], the models were trained for 200 epochs with a batch size of 32. For *Charades-STA* and *TVSum*, we used batch sizes of 32 and 4, respectively, with learning rates of $1e-4$ and $1e-3$. All experiments were conducted using T4 and RTX 3050 Ti GPUs.

A. Main Results

Performance in QVHighlights: In Table II, we compare the performance of various methods on the QVHighlights test split for both moment retrieval (MR) and highlight detection (HD) tasks. Our proposed framework, **VideoLights**, achieves state-of-the-art results across most metrics, demonstrating its robustness and effectiveness. Specifically, in the

TABLE III

EVALUATION OF HIGHLIGHT DETECTION METHODS ON TVSUM USING TOP-5 MAP. † REPRESENTS THE USE OF AUDIO MODALITY. ‡ INDICATES THE USE OF I3D FOR VISUAL FEATURES. HERE, BOLD REPRESENTS THE BEST RESULT, AND UNDERLINE REPRESENTS THE 2ND BEST RESULT.

Methods	VT	VU	GA	MS	PK	PR	FM	BK	BT	DS	Avg.
sLSTM [7]‡	41.1	46.2	46.3	47.7	44.8	46.1	45.2	40.6	47.1	45.5	45.1
SG [5]‡	42.3	47.2	47.5	48.9	45.6	47.3	46.4	41.7	48.3	46.6	46.2
LIM-S [76]‡	55.9	42.9	61.2	54.0	60.3	47.5	43.2	66.3	69.1	62.6	56.3
Trailer [77]‡	61.3	54.6	65.7	60.8	59.1	70.1	58.2	64.7	65.6	68.1	62.8
SL-Module [78]‡	86.5	68.7	74.9	86.2	79	63.2	58.9	72.6	78.9	64.0	73.3
UMT [17]†‡	87.5	81.5	81.5	81.5	81.4	87.0	76.0	86.9	84.4	79.6	83.1
QD-DETR [19]‡	88.2	87.4	85.6	85.0	85.8	86.9	76.4	91.3	<u>89.2</u>	73.7	85.0
UVCOM [62]‡	87.6	91.6	91.4	<u>86.7</u>	<u>86.9</u>	86.9	76.9	92.3	<u>87.4</u>	75.6	86.3
TR-DETR [22]‡	<u>89.3</u>	93.0	<u>94.3</u>	85.1	88.0	<u>88.6</u>	80.4	91.3	89.5	81.6	88.1
VideoLights †	89.8	<u>88.7</u>	95.0	88.0	83.6	90.1	<u>79.4</u>	94.2	88.6	<u>81.2</u>	<u>87.9</u>
UniVTG [20]	<u>83.9</u>	<u>85.1</u>	<u>89.0</u>	<u>80.1</u>	<u>84.6</u>	<u>81.4</u>	<u>70.9</u>	<u>91.7</u>	<u>73.5</u>	<u>69.3</u>	<u>81.0</u>
VideoLights	89.1	92.7	92.3	86.7	89.8	88.9	78.5	94.0	87.4	78.3	87.8
UniVTG (pt) [20]	92.0	77.8	89.8	83.8	<u>82.2</u>	<u>85.8</u>	74.3	91.8	90.5	77.6	84.6
VideoLights-pt	<u>90.8</u>	91.8	95.0	85.3	88.6	89.6	76.7	94.0	<u>88.5</u>	78.6	87.9
VideoLights-B	91.3	92.5	93.3	84.3	88.0	88.3	77.3	92.7	88.2	81.6	87.75
VideoLights-B-pt	91.4	88.2	93.0	95.2	87.2	89.1	76.1	95.1	88.6	81.3	88.52

MR task, our **VideoLights-B-pt** model achieves the highest R@0.5 (70.36), R@0.7 (55.25), mAP@0.5 (69.53), mAP@0.75 (49.17), and average mAP (47.94), surpassing all prior methods. Without pretraining, **VideoLights-B** also exhibits strong performance with R@0.5 (68.29), R@0.7 (52.79), mAP@0.5 (67.58), mAP@0.75 (47.30), and average mAP (46.53). These results indicate significant improvements over prior state-of-the-art methods like UVCOM and TR-DETR, with notable increases in R@0.5 (by 6.81% over UVCOM and 5.70% over TR-DETR) and average mAP (by 4.76% over UVCOM and 4.94% over TR-DETR). In the HD task, **VideoLights-B-pt** achieves an mAP of 42.84 and HIT@1 of 70.56, outperforming other methods by considerable margins. Similarly, **VideoLights-B** delivers strong results, with an mAP of 42.43 and HIT@1 of 68.94, maintaining a lead over both UVCOM and UniVTG. Even with fewer features, our models (**VideoLights** and **VideoLights-pt**) achieve competitive results, highlighting the flexibility and scalability of our approach. For instance, **VideoLights-pt** achieves the second-highest R@0.5 (68.48) and R@0.7 (52.53), as well as competitive mAP scores, demonstrating its effectiveness even in pretraining fine-tuning settings. These improvements, ranging from 2.76% to 7.07% across various metrics, underscore the superiority of our framework in both moment retrieval and highlight detection tasks. The integration of additional features (e.g., BLIP) further enhances performance, showing the potential of our framework for video-language understanding tasks.

Performance in Charades-STA: Our proposed models, **VideoLights**, **VideoLights-pt**, **VideoLights-B**, and **VideoLights-B-pt**, demonstrate strong performance on the Charades-STA test set (Table IV). Without pretraining, **VideoLights** achieves state-of-the-art results in three of the four metrics. It outperforms UniVTG in R@0.5 by 0.03% (58.04 vs 58.01) and in R@0.7 by 1.23% (36.88 vs 35.65), while achieving comparable mIoU with a 0.1% improvement (50.20 vs 50.10). How-

TABLE IV

RESULTS ON CHARADES-STA TEST SET. HERE, BOLD REPRESENTS THE BEST RESULT, AND UNDERLINE REPRESENTS THE 2ND BEST RESULT.

Method	R@0.3	R@0.5	R@0.7	mIoU
2D-TAN [35]	58.76	46.02	27.5	41.25
VSLNet [48]	60.30	42.69	24.14	41.58
Moment-DETR [16]	65.83	52.07	30.59	45.54
QD-DETR [19]	-	57.31	32.55	-
TR-DETR [22]	-	57.61	33.52	-
UniVTG [20]	70.81	58.01	35.65	50.10
VideoLights	<u>70.67</u>	58.04	36.88	50.20
UniVTG (pt) [20]	72.63	60.19	38.55	52.17
VideoLights-pt	<u>72.26</u>	<u>60.11</u>	<u>37.80</u>	<u>51.44</u>
VideoLights-B	71.72	60.30	37.23	51.25
VideoLights-B-pt	73.33	61.96	41.05	52.94

ever, for R@0.3, **VideoLights** slightly trails UniVTG by 0.14% (70.67 vs 70.81). In the pretraining setting, **VideoLights-pt** shows competitive results, closely trailing UniVTG (pt) in all metrics. **VideoLights-pt** achieves 72.26 in R@0.3, 60.11 in R@0.5, 37.80 in R@0.7, and 51.44 in mIoU, compared to UniVTG (pt)'s 72.63, 60.19, 38.55, and 52.17, respectively. Additionally, our new models, **VideoLights-B** and **VideoLights-B-pt**, incorporating BLIP features, exhibit superior performance. Without pretraining, **VideoLights-B** surpasses UniVTG in R@0.5 (60.30 vs 58.01) and mIoU (51.25 vs 50.10), though it slightly lags in R@0.3 (71.72 vs 70.81) and R@0.7 (37.23 vs 35.65). With pretraining, **VideoLights-B-pt** sets a new state-of-the-art across all metrics, achieving 73.33 in R@0.3, 61.96 in R@0.5, 41.05 in R@0.7, and 52.94 in mIoU, surpassing UniVTG (pt) by 0.70%, 1.77%, 2.50%, and 0.77%, respectively. These results highlight the efficacy of our approach, particularly with the integration of BLIP features and in pretraining scenarios, significantly advancing performance across all evaluation criteria.

Performance in TVSum: Our proposed model, **VideoLights**, demonstrates competitive performance

TABLE V

ABLATION STUDY ON QVHIGHLIGHTS VAL SPLIT. FRA STANDS FOR FRA MODULE, BI STANDS FOR BI-CMF MODULE, BF STANDS FOR BLIP FEATURES, PT STANDS FOR PRE-TRAIN ON THE SYNTHETIC DATASET USING BLIP BACKEND, HL STANDS FOR ADAPTIVE HARD POSITIVE AND NEGATIVE LOSS, TCL STANDS FOR TASK COUPLED LOSS, SCSL STANDS FOR SALIENCY COSINE SIMILARITY LOSS, AND AL STANDS FOR ALIGNMENT LOSS. THE EFFECT OF DIFFERENT PRETRAINING DATA IS IN THE BOTTOM BLOCK WITHOUT ANY NEW LOSSES.

sl.	Modules				Losses				MR				HD		
									R1		mAP		>=Very Good		
	fra	bi	bf	pt	hl	tcl	scsl	al	@0.5	@0.7	@0.5	@0.75	Avg	mAP	HIT@1
1.	X	X	X	X	✓	✓	✓	✓	61.42	46.77	60.82	41.36	41.28	38.08	60.45
2.	X	X	✓	X	✓	✓	✓	✓	64.45	49.48	63.69	43.08	43.28	39.98	64.13
3.	✓	✓	X	X	✓	✓	✓	✓	66.77	51.23	65.83	45.38	45.12	40.74	66.9
4.	X	✓	✓	X	✓	✓	✓	✓	65.42	52.84	64.89	46.67	45.69	40.75	65.55
5.	✓	X	✓	X	✓	✓	✓	✓	69.55	53.94	67.53	47.86	47.14	42.09	68.77
6.	✓	✓	✓	X	✓	✓	✓	✓	70.06	55.35	68.75	49.22	48.44	42.84	70.71
7.	✓	✓	✓	X	X	X	X	X	69.55	54.39	68.34	49.0	47.32	41.96	68.06
8.	✓	✓	✓	X	✓	X	X	X	70.19	54.77	68.59	49.00	48.35	42.73	69.10
9.	✓	✓	✓	X	X	✓	X	X	69.55	54.00	68.37	47.80	47.63	41.85	69.61
10.	✓	✓	✓	X	X	X	X	X	69.81	54.39	69.06	49.21	48.56	42.76	69.74
11.	✓	✓	✓	X	X	X	X	✓	69.68	54.71	67.80	47.80	54.71	41.79	68.26
12.	✓	✓	X	✓	✓	✓	✓	✓	71.03	54.84	68.07	47.36	46.06	42.16	69.16
13.	✓	✓	✓	✓	✓	✓	✓	✓	72.06	57.94	70.38	51.12	49.71	43.12	71.48
No Pretraining									66.77	51.23	65.83	45.38	45.12	40.74	66.9
ASR Pretraining [16]									67.94	51.48	65.84	44.03	43.74	40.71	67.03
Our BLIP Pretraining									71.03	54.84	68.07	47.36	46.06	42.16	69.16

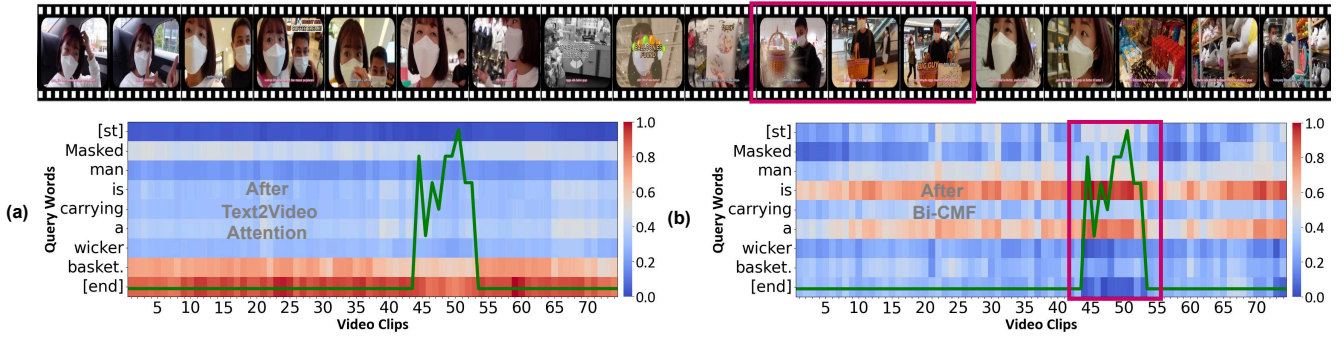


Fig. 5. (a) and (b) show video-query correspondence maps: (a) after text-to-video (t2v) attention and (b) after the Bi-CMF layer. The green line represents the ground truth saliency scores. Bi-CMF attends to the correct video region better than t2v (highlighted in the magenta box). The word ‘is’ asserts that ‘a’ refers to one basket, unlike ‘is not’.

across various domains in the TVSum dataset, as shown in Table III. **VideoLights** achieves state-of-the-art results in 5 out of 10 domains and in the overall average. Specifically, it outperforms previous methods in VT (89.8% vs. TR-DETR’s 89.3%, a 0.56% improvement), GA (95.0% vs. TR-DETR’s 94.3%, a 0.74% increase), MS (88.0% vs. TR-DETR’s 85.1%, a 3.41% gain), PR (90.1% vs. TR-DETR’s 88.6%, a 1.69% improvement), and BK (94.2% vs. TR-DETR’s 91.3%, a 3.18% improvement). In other domains, **VideoLights** shows highly competitive performance: VU (88.7% vs. TR-DETR’s 93.0%, -4.62%), PK (83.6% vs. TR-DETR’s 88.0%, -5.00%), FM (79.4% vs. TR-DETR’s 80.4%, -1.24%), BT (88.6% vs. TR-DETR’s 89.5%, -1.01%), and DS (81.2% vs. TR-DETR’s 81.6%, -0.49%). Notably, **VideoLights** achieves an overall average of 87.9%, closely trailing TR-DETR’s 88.1% by 0.23%. When compared with UniVTG, our models **VideoLights** and **VideoLights-pt**, trained with SlowFast and CLIP, demonstrate significant improvements across most domains. **VideoLights** achieves an overall average of 87.9%, surpassing UniVTG’s

81.0% by 6.9%. It consistently outperforms UniVTG in all domains, with notable gains in VU (92.7% vs. 85.1%, a 7.6% improvement), GA (92.3% vs. 89.0%, a 3.7% improvement), and MS (86.7% vs. 80.1%, a 6.6% improvement). Similarly, **VideoLights-pt** demonstrates superior performance over UniVTG (pt), achieving an overall average of 87.9% compared to 84.6%, a 3.3% improvement. It achieves state-of-the-art results in 7 out of 10 domains, including GA (95.0% vs. UniVTG (pt)’s 89.8%, a 5.8% gain), MS (85.3% vs. 83.8%, a 1.5% gain), and BK (94.0% vs. 91.8%, a 2.2% improvement). When comparing the models incorporating BLIP features, **VideoLights-B** achieves competitive results, notably excelling in domains such as VU (92.5%), BK (92.7%), and DS (81.6%), achieving an average of 87.75%. Additionally, the pretraining-enhanced version, **VideoLights-pt**, achieves the best overall average performance at 87.9%, surpassing UniVTG (pt)’s 84.6% by 3.3%. It secures state-of-the-art results in 7 domains, including VU (91.8%), GA (95.0%), MS (85.3%), PK (88.6%), PR (89.6%), BK (94.0%), and DS (78.6%). These results highlight the effectiveness of

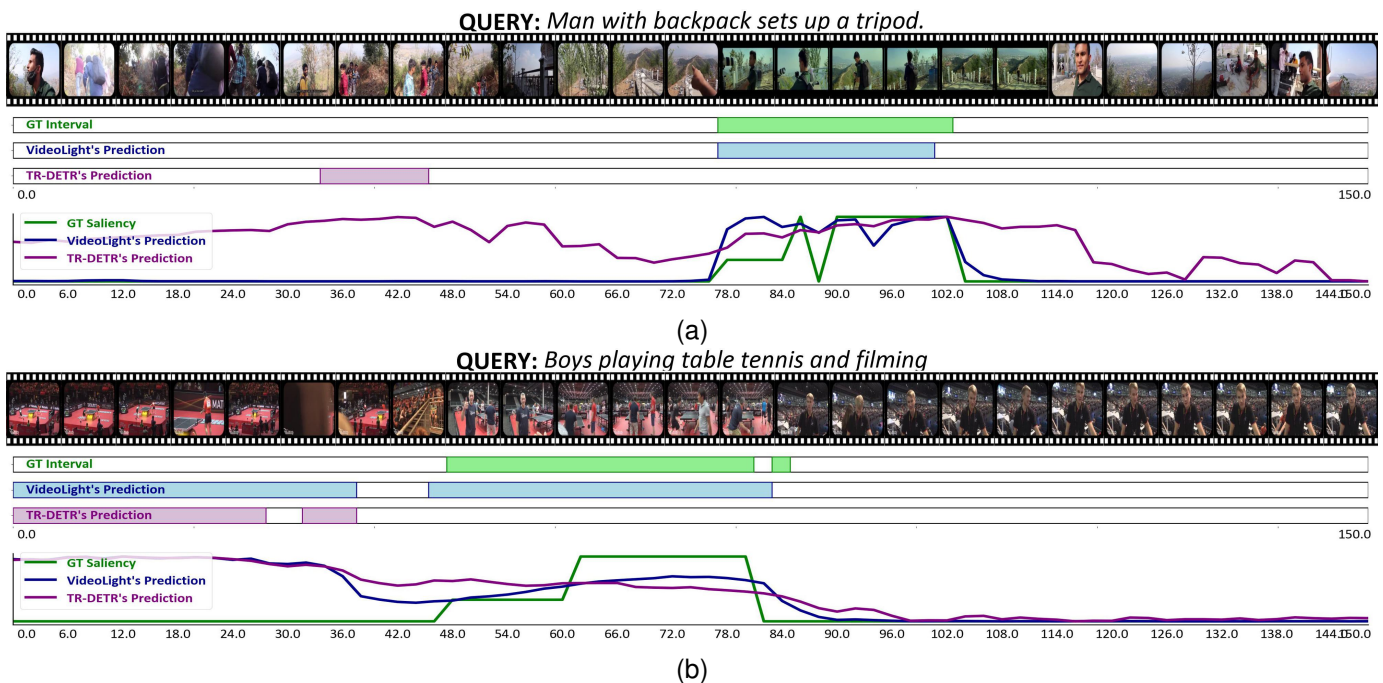


Fig. 6. Qualitative results. (a) demonstrates **VideoLights** outperformed TR-DETR [22] in both MR and HD. (b) Both **VideoLights** and TR-DETR performed below the ground truth, but upon closer examination, it is evident that incorrectly predicted clips are still related to the given query.

TABLE VI
EFFECT OF BI-CMF VS UNI-CMF ON **VideoLights** ON QVHIGHLIGHTS VAL SET

Cross-Attention Type	MR			HD	
	R1@0.5	R1@0.75	mAP@Avg	mAP	HIT@1
Bi-CMF	70.06	55.35	48.44	42.84	70.71
Uni-CMF	69.55	53.94	47.14	42.09	68.77

TABLE VII
EFFECT OF FRA ON DIFFERENT METHODS ON QVHIGHLIGHTS VAL SET. † REPRESENTS THE USE OF THE FRA MODULE

Method	MR			HD	
	R1@0.5	R1@0.75	mAP@Avg	mAP	HIT@1
Moment-DETR [16]	53.94	34.84	32.2	35.36	55.55
Moment-DETR †	61.48	40.26	35.17	38.88	63.16
QD-DETR [19]	62.68	46.66	41.22	39.13	63.03
QD-DETR †	63.81	46.84	41.71	39.77	63.87
TR-DETR [22]	67.1	51.48	45.09	40.55	64.77
TR-DETR †	67.81	51.68	45.19	41.37	67.03

VideoLights and its variants in video highlight detection tasks, achieving state-of-the-art performance in key domains while maintaining competitive results across others.

In summary, **VideoLights** not only matches but often exceeds the performance of other cutting-edge methods, demonstrating its effectiveness in joint video highlight detection & moment retrieval. Along with the quantitative results, Fig. 6 shows the qualitative results on the QVHighlights dataset.

B. Ablation Studies

To comprehend module impacts, we present our model ablation on QVHighlights val split in Table V.

TABLE VIII
EFFECT OF INTEGRATING FEATURES FROM DIFFERENT VLM'S ON **VideoLights** ON QVHIGHLIGHTS VAL SET. HERE SF STANDS FOR SLOWFAST, C STANDS FOR CLIP, AND B STANDS FOR BLIP-2.

Feature type	MR			HD	
	R1@0.5	R1@0.75	mAP@Avg	mAP	HIT@1
SF + C	66.77	51.23	45.12	40.74	66.9
SF + B	69.23	53.42	46.86	42.20	69.68
SF + C + B	70.06	55.35	48.44	42.84	70.71

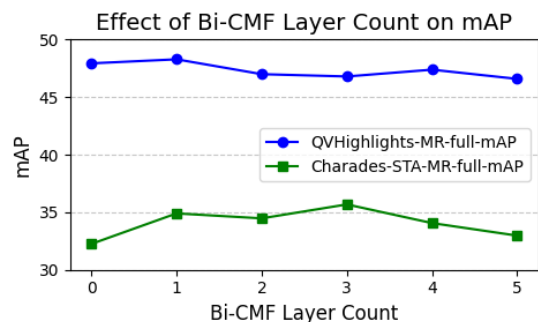


Fig. 7. Empirical analysis reveals optimal Bi-CMF performance varies across datasets: three layers yielded superior results on one benchmark, while a single layer demonstrated peak performance on another. Consequently, we adopted a layer count of one for Bi-CMF across both datasets to ensure consistent cross-modal alignment.

Effect of FRA: From Table V comparing rows 2 and 5, the addition of the FRA module while keeping Bi-CMF disabled results in an average performance gain of 7.93% across all metrics with a minimum 5.28% and a maximum 11.09%. Also, Fig. 3 shows the qualitative efficacy of this module. We have done additional experiments, adding FRA to other existing methods and the results are shown in Table VII.

The FRA module consistently enhances performance across methods, with significant improvements for weaker baselines like Moment-DETR and incremental gains for stronger models like QD-DETR and TR-DETR.

Effect of Bi-CMF: The rows 2 and 4 of Table V demonstrate the effectiveness of our *Bi-CMF* module, showing an average performance gain of 4.03% across all metrics, with the most significant improvement in mAP@0.75 (8.33%). A qualitative analysis through feature heatmap visualization in Fig. 5 reveals that *Bi-CMF* achieves a more sparse spectrum density compared to both baseline (no cross-modal) and uni-directional (text-to-video) cross-modal fusion (Uni-CMF) approaches like QD-DETR, indicating better query relevance differentiation. From Table VI we see, Bi-CMF consistently outperforms Uni-CMF across all metrics, with the most significant improvements seen in HIT@1 (+1.94) and R1@0.75 (+1.41). This demonstrates the effectiveness of Bi-CMF over Uni-CMF.

Effect of new loss functions: Rows 6 to 11 in Table V illustrate the performance enhancements achieved through the integration of our proposed loss functions: adaptive hard positive and negative loss (hl), task-coupled loss (tcl), saliency cosine similarity loss (scsl), and alignment loss (al). Each loss function independently contributes to the improvement of both Moment Retrieval (MR) and Highlight Detection (HD) tasks. Notably, hl results in advancements in metrics such as MR R1@0.5 and HD HIT@1, tcl enhances performance in MR mAP@0.75, and scsl yields balanced gains across all metrics. The introduction of al further sharpens the outcomes, especially in HD HIT@1. Although each loss demonstrates its effectiveness when utilized individually, the combination of all losses in Row 6 achieves the best overall performance, underscoring the synergistic benefit of employing all loss functions collectively.

Effect of Blip-2 features and Pretraining: As shown, especially the difference between the 6th row and the 11th row in Table V in the upper block, pre-training also helps improve performance. The usage of BLIP-2 features, along with the standard CLIP and SlowFast, also brings about improvements. We have run additional experiments to check the effectiveness of each feature. From Table VIII we see that using BLIP-2 feature replacing CLIP results in performance improvement. But it achieves the best results when SlowFast, CLIP, and BLIP-2 are being used together. The bottom block of Table V shows the results with different pretraining corpora that pose the effectiveness of pretraining. For this experiment, SlowFast and CLIP features were used, and we kept all modules and losses. Here we see that BLIP Pretraing has a minimum 3.18% to a maximum 7.57% performance gain on ASR Pretraining.

V. LIMITATION AND CONCLUSION

Conclusion: In this paper, we introduce **VideoLights**, a novel framework that jointly tackles the challenges of video highlight detection (HD) and moment retrieval (MR). By harnessing the interplay between text and video modalities through innovative cross-task and cross-modal interactions, **VideoLights** achieves state-of-the-art performance on benchmark datasets, including QVHighlights, TVSum, and

Charades-STA. Key contributions of this framework include the Feature Refinement and Alignment (FRA) module, which facilitates effective local and global feature alignment; the Bi-Directional Cross-Modal Fusion (Bi-CMF) network that enhances query-aware representations; and the Unidirectional Joint-Task Feedback Mechanism (Uni-JFM), which optimizes both task-specific and cross-task learning efficiency. We leverage features from Large Vision-Language Models (LVLMs) like BLIP-2 to enhance temporal awareness, ensure semantic alignment, and integrate multimodal features effectively. Additionally, we employ intelligent synthetic data generation using LVLMs and pre-training techniques to boost performance and robustness. The adaptive error correction mechanism further ensures accurate predictions of clip saliency. Comprehensive evaluations and ablation studies substantiate the effectiveness of **VideoLights**, demonstrating its consistent superiority over previous baselines across various metrics. Future research could delve into advancements in multimodal fusion techniques, improved feature alignment and refinement methods, and broader applications within real-world video platforms. While LVLMs exhibit great potential in multimodal reasoning, their effectiveness in moment retrieval tasks merits further exploration. We contend that **VideoLights** establishes a solid foundation for progressing joint HD/MR prediction, paving the way for scalable and precise video understanding systems.

Limitation: Our proposal for weakly supervised pre-training utilizing vision-language pretraining models simplifies the training process but may still be prone to biases or inaccuracies in caption generation. At the same time, our dependency on pretraining models for caption generation and feature extraction can lead to computational overhead and reliance on external resources, thus potentially limiting the scalability of our approach. Moreover, the performance of our Bi-CMF module is heavily reliant on the quality of input features and the effectiveness of attention mechanisms, both of which can vary depending on the complexity and diversity of the video content. To fully unlock the potential of our proposed approach in real-world applications, it is crucial to address these limitations through further research and refinement.

REFERENCES

- [1] E. Apostolidis, E. Adamantidou, A. I. Metsai, V. Mezaris, and I. Patras, "Video summarization using deep neural networks: A survey," *Proceedings of the IEEE*, vol. 109, no. 11, pp. 1838–1863, 2021.
- [2] Z. Wu, T. Yao, Y. Fu, and Y.-G. Jiang, *Deep learning for video classification and captioning*. Kentfield, CA: Association for Computing Machinery and Morgan & Claypool, Dec. 2017, p. 3–29.
- [3] L. Anne Hendricks, O. Wang, E. Shechtman, J. Sivic, T. Darrell, and B. Russell, "Localizing moments in video with natural language," in *Proceedings of the IEEE international conference on computer vision*. Venice, Italy: IEEE, 2017, pp. 5803–5812.
- [4] T. Badamjorj, M. Rochan, Y. Wang, and L. Cheng, "Contrastive learning for unsupervised video highlight detection," in *Proceedings of the IEEE/CVF Conference on Computer Vision and Pattern Recognition*. New Orleans, Louisiana, USA: IEEE/CVF, 2022, pp. 14 042–14 052.
- [5] B. Mahasseni, M. Lam, and S. Todorovic, "Unsupervised video summarization with adversarial lstm networks," in *Proceedings of the IEEE conference on Computer Vision and Pattern Recognition*. Honolulu, Hawaii, USA: IEEE, 2017, pp. 202–211.

- [6] F. Wei, B. Wang, T. Ge, Y. Jiang, W. Li, and L. Duan, "Learning pixel-level distinctions for video highlight detection," in *Proceedings of the IEEE/CVF Conference on Computer Vision and Pattern Recognition*. New Orleans, Louisiana, USA: IEEE/CVF, 2022, pp. 3073–3082.
- [7] K. Zhang, W.-L. Chao, F. Sha, and K. Grauman, "Video summarization with long short-term memory," in *Computer Vision—ECCV 2016: 14th European Conference, October 11–14, 2016, Proceedings, Part VII 14*, Springer. Amsterdam, The Netherlands: Springer International Publishing, 2016, pp. 766–782.
- [8] J. Chen, J. Wang, X. Wang, X. Wang, Z. Feng, R. Liu, and M. Song, "Coevo-net: Coevolution network for video highlight detection," *IEEE Transactions on Circuits and Systems for Video Technology*, vol. 32, no. 6, pp. 3788–3797, 2022.
- [9] J. Gao, C. Sun, Z. Yang, and R. Nevatia, "Tall: Temporal activity localization via language query," in *Proceedings of the IEEE international conference on computer vision*. Venice, Italy: IEEE, 2017, pp. 5267–5275.
- [10] W. Liu, T. Mei, Y. Zhang, C. Che, and J. Luo, "Multi-task deep visual-semantic embedding for video thumbnail selection," in *Proceedings of the IEEE conference on computer vision and pattern recognition*. Boston, Massachusetts, USA: IEEE, 2015, pp. 3707–3715.
- [11] V. Escorcia, M. Soldan, J. Sivic, B. Ghanem, and B. Russell, "Finding moments in video collections using natural language," 2022.
- [12] D. Han, X. Cheng, N. Guo, X. Ye, B. Rainer, and P. Priller, "Momentum cross-modal contrastive learning for video moment retrieval," *IEEE Transactions on Circuits and Systems for Video Technology*, vol. 34, no. 7, pp. 5977–5994, 2024.
- [13] X. Sun, J. Gao, Y. Zhu, X. Wang, and X. Zhou, "Video moment retrieval via comprehensive relation-aware network," *IEEE Transactions on Circuits and Systems for Video Technology*, vol. 33, no. 9, pp. 5281–5295, 2023.
- [14] J. Gao and C. Xu, "Learning video moment retrieval without a single annotated video," *IEEE Transactions on Circuits and Systems for Video Technology*, vol. 32, no. 3, pp. 1646–1657, 2022.
- [15] H. Tang, J. Zhu, M. Liu, Z. Gao, and Z. Cheng, "Frame-wise cross-modal matching for video moment retrieval," *IEEE Transactions on Multimedia*, vol. 24, pp. 1338–1349, 2022.
- [16] J. Lei, T. L. Berg, and M. Bansal, "Detecting moments and highlights in videos via natural language queries," *Advances in Neural Information Processing Systems*, vol. 34, pp. 11 846–11 858, 2021.
- [17] Y. Liu, S. Li, Y. Wu, C.-W. Chen, Y. Shan, and X. Qie, "Umt: Unified multi-modal transformers for joint video moment retrieval and highlight detection," in *Proceedings of the IEEE/CVF Conference on Computer Vision and Pattern Recognition (CVPR)*. New Orleans, Louisiana, USA: IEEE/CVF, June 2022, pp. 3042–3051.
- [18] J. Yang, P. Wei, H. Li, and Z. Ren, "Task-driven exploration: Decoupling and inter-task feedback for joint moment retrieval and highlight detection," in *Proceedings of the IEEE/CVF Conference on Computer Vision and Pattern Recognition (CVPR)*, June 2024, pp. 18 308–18 318.
- [19] W. Moon, S. Hyun, S. Park, D. Park, and J.-P. Heo, "Query-dependent video representation for moment retrieval and highlight detection," in *Proceedings of the IEEE/CVF Conference on Computer Vision and Pattern Recognition (CVPR)*. Vancouver Canada: IEEE/CVF, June 2023, pp. 23 023–23 033.
- [20] K. Q. Lin, P. Zhang, J. Chen, S. Pramanick, D. Gao, A. J. Wang, R. Yan, and M. Z. Shou, "Univtg: Towards unified video-language temporal grounding," in *Proceedings of the IEEE/CVF International Conference on Computer Vision*. Paris, France: IEEE/CVF, 2023, pp. 2794–2804.
- [21] J. Jang, J. Park, J. Kim, H. Kwon, and K. Sohn, "Knowing where to focus: Event-aware transformer for video grounding," in *Proceedings of the IEEE/CVF International Conference on Computer Vision*. Paris, France: IEEE/CVF, 2023, pp. 13 846–13 856.
- [22] H. Sun, M. Zhou, W. Chen, and W. Xie, "Tr-detr: Task-reciprocal transformer for joint moment retrieval and highlight detection," *Proceedings of the AAAI Conference on Artificial Intelligence*, vol. 38, no. 5, pp. 4998–5007, Mar. 2024.
- [23] R. Wang, J. Feng, F. Zhang, X. Luo, and Y. Luo, "Modality-aware heterogeneous graph for joint video moment retrieval and highlight detection," *IEEE Transactions on Circuits and Systems for Video Technology*, vol. 34, no. 9, pp. 8896–8911, 2024.
- [24] A. Radford, J. W. Kim, C. Hallacy, A. Ramesh, G. Goh, S. Agarwal, G. Sastry, A. Askell, P. Mishkin, J. Clark *et al.*, "Learning transferable visual models from natural language supervision," in *International conference on machine learning*, PMLR. Virtual: PMLR, 2021, pp. 8748–8763.
- [25] J. Li, D. Li, C. Xiong, and S. Hoi, "Blip: Bootstrapping language-image pre-training for unified vision-language understanding and generation," in *International conference on machine learning*, PMLR. Baltimore MD: PMLR, 2022, pp. 12 888–12 900.
- [26] W. Kay, J. Carreira, K. Simonyan, B. Zhang, C. Hillier, S. Vijayanarasimhan, F. Viola, T. Green, T. Back, P. Natsev, M. Suleyman, and A. Zisserman, "The kinetics human action video dataset," 2017.
- [27] C. Feichtenhofer, H. Fan, J. Malik, and K. He, "Slowfast networks for video recognition," in *Proceedings of the IEEE/CVF international conference on computer vision*. Seoul, Korea: IEEE/CVF, 2019, pp. 6202–6211.
- [28] Z. Yang, L. Li, K. Lin, J. Wang, C. Lin, Z. Liu, and L. Wang, "The dawn of lmms: Preliminary explorations with gpt-4v(ision)," *CoRR*, vol. abs/2309.17421, 2023.
- [29] H. Liu, C. Li, Q. Wu, and Y. J. Lee, "Visual instruction tuning," *Advances in neural information processing systems*, vol. 36, 2024.
- [30] J. Li, D. Li, S. Savarese, and S. Hoi, "Blip-2: Bootstrapping language-image pre-training with frozen image encoders and large language models," in *International conference on machine learning*, PMLR. Honolulu, HI: PMLR, 2023, pp. 19 730–19 742.
- [31] Y. Jiang, X. Yan, G.-P. Ji, K. Fu, M. Sun, H. Xiong, D.-P. Fan, and F. S. Khan, "Effectiveness assessment of recent large vision-language models," *Visual Intelligence*, vol. 2, no. 1, Jun. 2024.
- [32] Y. Song, J. Vallmitjana, A. Stent, and A. Jaimes, "Tvsun: Summarizing web videos using titles," in *Proceedings of the IEEE conference on computer vision and pattern recognition*. Boston, Massachusetts, USA: IEEE, 2015, pp. 5179–5187.
- [33] L. A. Hendricks, O. Wang, E. Shechtman, J. Sivic, T. Darrell, and B. Russell, "Localizing moments in video with temporal language," in *Proceedings of the 2018 Conference on Empirical Methods in Natural Language Processing*. Brussels, Belgium: Association for Computational Linguistics, Oct.-Nov. 2018, pp. 1380–1390.
- [34] Y. Zeng, D. Cao, X. Wei, M. Liu, Z. Zhao, and Z. Qin, "Multi-modal relational graph for cross-modal video moment retrieval," in *Proceedings of the IEEE/CVF conference on computer vision and pattern recognition*, 2021, pp. 2215–2224.
- [35] S. Zhang, H. Peng, J. Fu, and J. Luo, "Learning 2d temporal adjacent networks for moment localization with natural language," *Proceedings of the AAAI Conference on Artificial Intelligence*, vol. 34, no. 07, pp. 12 870–12 877, Apr. 2020.
- [36] S. Xiao, L. Chen, S. Zhang, W. Ji, J. Shao, L. Ye, and J. Xiao, "Boundary proposal network for two-stage natural language video localization," in *Proceedings of the AAAI Conference on Artificial Intelligence*, vol. 35, 2021, pp. 2986–2994.
- [37] J. Chen, X. Chen, L. Ma, Z. Jie, and T.-S. Chua, "Temporally grounding natural sentence in video," in *Proceedings of the 2018 conference on empirical methods in natural language processing*, 2018, pp. 162–171.
- [38] D. Liu, X. Qu, J. Dong, and P. Zhou, "Reasoning step-by-step: Temporal sentence localization in videos via deep rectification-modulation network," in *Proceedings of the 28th International Conference on Computational Linguistics*, 2020, pp. 1841–1851.
- [39] X. Qu, P. Tang, Z. Zou, Y. Cheng, J. Dong, P. Zhou, and Z. Xu, "Fine-grained iterative attention network for temporal language localization in videos," in *Proceedings of the 28th ACM International Conference on Multimedia*, 2020, pp. 4280–4288.
- [40] K. Ning, L. Xie, J. Liu, F. Wu, and Q. Tian, "Interaction-integrated network for natural language moment localization," *IEEE Transactions on Image Processing*, vol. 30, pp. 2538–2548, 2021.
- [41] Y. Yuan, L. Ma, J. Wang, W. Liu, and W. Zhu, "Semantic conditioned dynamic modulation for temporal sentence grounding in videos," *Advances in Neural Information Processing Systems*, vol. 32, 2019.
- [42] D. Zhang, X. Dai, X. Wang, Y.-F. Wang, and L. S. Davis, "Man: Moment alignment network for natural language moment retrieval via iterative graph adjustment," in *Proceedings of the IEEE/CVF Conference on Computer Vision and Pattern Recognition*, 2019, pp. 1247–1257.
- [43] Y. Zhao, Z. Zhao, Z. Zhang, and Z. Lin, "Cascaded prediction network via segment tree for temporal video grounding," in *Proceedings of the IEEE/CVF Conference on Computer Vision and Pattern Recognition*, 2021, pp. 4197–4206.
- [44] S. Xiao, L. Chen, J. Shao, Y. Zhuang, and J. Xiao, "Natural language video localization with learnable moment proposals," in *Proceedings of the 2021 Conference on Empirical Methods in Natural Language Processing*. Online and Punta Cana, Dominican Republic: Association for Computational Linguistics, Nov. 2021, pp. 4008–4017.
- [45] B. Liu, S. Yeung, E. Chou, D.-A. Huang, L. Fei-Fei, and J. C. Niebles, "Temporal modular networks for retrieving complex compositional activities in videos," in *Proceedings of the European Conference on Computer Vision (ECCV)*, 2018, pp. 552–568.

- [46] M. Zhang, Y. Yang, X. Chen, Y. Ji, X. Xu, J. Li, and H. T. Shen, "Multi-stage aggregated transformer network for temporal language localization in videos," in *Proceedings of the IEEE/CVF Conference on Computer Vision and Pattern Recognition*, 2021, pp. 12 669–12 678.
- [47] H. Wang, Z.-J. Zha, L. Li, D. Liu, and J. Luo, "Structured multi-level interaction network for video moment localization via language query," in *Proceedings of the IEEE/CVF Conference on Computer Vision and Pattern Recognition*, 2021, pp. 7026–7035.
- [48] H. Zhang, A. Sun, W. Jing, and J. T. Zhou, "Span-based localizing network for natural language video localization," in *Proceedings of the 58th Annual Meeting of the Association for Computational Linguistics*. Online: Association for Computational Linguistics, Jul. 2020, pp. 6543–6554.
- [49] J. Mun, M. Cho, and B. Han, "Local-global video-text interactions for temporal grounding," in *Proceedings of the IEEE/CVF Conference on Computer Vision and Pattern Recognition*, 2020, pp. 10 810–10 819.
- [50] D. Liu, X. Qu, J. Dong, P. Zhou, Y. Cheng, W. Wei, Z. Xu, and Y. Xie, "Context-aware biaffine localization network for temporal sentence grounding," in *Proceedings of the IEEE/CVF Conference on Computer Vision and Pattern Recognition*, 2021, pp. 11 235–11 244.
- [51] R. Zeng, H. Xu, W. Huang, P. Chen, M. Tan, and C. Gan, "Dense regression network for video grounding," in *Proceedings of the IEEE/CVF Conference on Computer Vision and Pattern Recognition*, 2020, pp. 10 287–10 296.
- [52] A. Vaswani, N. Shazeer, N. Parmar, J. Uszkoreit, L. Jones, A. N. Gomez, L. u. Kaiser, and I. Polosukhin, "Attention is all you need," in *Advances in Neural Information Processing Systems*, vol. 30. Long Beach, California: Curran Associates, Inc., 2017.
- [53] N. Carion, F. Massa, G. Synnaeve, N. Usunier, A. Kirillov, and S. Zagoruyko, "End-to-end object detection with transformers," in *European conference on computer vision*, Springer. Tel Aviv, Israel: Springer International Publishing, 2020, pp. 213–229.
- [54] J. Lei, L. Yu, T. L. Berg, and M. Bansal, "Tvr: A large-scale dataset for video-subtitle moment retrieval," in *Computer Vision—ECCV 2020: 16th European Conference, August 23–28, 2020, Proceedings, Part XXI 16*, Springer. Glasgow, UK: Springer International Publishing, 2020, pp. 447–463.
- [55] J. Gao and C. Xu, "Fast video moment retrieval," in *Proceedings of the IEEE/CVF International Conference on Computer Vision*. Virtual: IEEE/CVF, 2021, pp. 1523–1532.
- [56] Y. Liu, J. He, W. Li, J. Kim, D. Wei, H. Pfister, and C. W. Chen, " r^2 -tuning: Efficient image-to-video transfer learning for video temporal grounding," in *Proceedings of the European Conference on Computer Vision (ECCV)*, 2024.
- [57] N. Messina, G. Amato, A. Esuli, F. Falchi, C. Gennaro, and S. Marchand-Maillet, "Fine-grained visual textual alignment for cross-modal retrieval using transformer encoders," *ACM Transactions on Multimedia Computing, Communications, and Applications (TOMM)*, vol. 17, no. 4, pp. 1–23, 2021.
- [58] J. Hu, S. Qian, Q. Fang, and C. Xu, "Hierarchical graph semantic pooling network for multi-modal community question answer matching," in *Proceedings of the 27th ACM International Conference on Multimedia*. Nice, France: ACM, 2019, pp. 1157–1165.
- [59] P. Morgado, Y. Li, and N. Nvasconcelos, "Learning representations from audio-visual spatial alignment," *Advances in Neural Information Processing Systems*, vol. 33, pp. 4733–4744, 2020.
- [60] T. Badamdorj, M. Rochan, Y. Wang, and L. Cheng, "Joint visual and audio learning for video highlight detection," in *Proceedings of the IEEE/CVF International Conference on Computer Vision*, 2021, pp. 8127–8137.
- [61] S. Yan, X. Xiong, A. Nagrani, A. Arnab, Z. Wang, W. Ge, D. Ross, and C. Schmid, "Unloc: A unified framework for video localization tasks," in *Proceedings of the IEEE/CVF International Conference on Computer Vision (ICCV)*. Paris, France: IEEE/CVF, October 2023, pp. 13 623–13 633.
- [62] Y. Xiao, Z. Luo, Y. Liu, Y. Ma, H. Bian, Y. Ji, Y. Yang, and X. Li, "Bridging the gap: A unified video comprehension framework for moment retrieval and highlight detection," in *Proceedings of the IEEE/CVF Conference on Computer Vision and Pattern Recognition*, 2024, pp. 18 709–18 719.
- [63] J. Carreira, E. Noland, C. Hillier, and A. Zisserman, "A short note on the kinetics-700 human action dataset," 2022.
- [64] K. Grauman, A. Westbury, E. Byrne, Z. Chavis, A. Furnari, R. Girdhar, J. Hamburger, H. Jiang, M. Liu, X. Liu *et al.*, "Ego4d: Around the world in 3,000 hours of egocentric video," in *Proceedings of the IEEE/CVF Conference on Computer Vision and Pattern Recognition*. New Orleans, Louisiana, USA: IEEE/CVF, 2022, pp. 18 995–19 012.
- [65] A. Nagrani, P. H. Seo, B. Seybold, A. Hauth, S. Manen, C. Sun, and C. Schmid, "Learning audio-video modalities from image captions," in *European Conference on Computer Vision*, Springer. Tel Aviv: Springer, 2022, pp. 407–426.
- [66] M. R. Parvez, J. Chi, W. U. Ahmad, Y. Tian, and K.-W. Chang, "Retrieval enhanced data augmentation for question answering on privacy policies," in *Proceedings of the 17th Conference of the European Chapter of the Association for Computational Linguistics*. Dubrovnik, Croatia: Association for Computational Linguistics, May 2023, pp. 201–210.
- [67] G. I. O. Union, "A metric and a loss for bounding box regression," in *Proceedings of the IEEE/CVF Conference on Computer Vision and Pattern Recognition (CVPR)*. Long Beach, CA, USA: IEEE/CVF, 2019, pp. 658–666.
- [68] K. He, X. Zhang, S. Ren, and J. Sun, "Deep residual learning for image recognition," in *Proceedings of the IEEE conference on computer vision and pattern recognition*. LAS VEGAS, USA: IEEE, 2016, pp. 770–778.
- [69] J. L. Ba, J. R. Kiros, and G. E. Hinton, "Layer normalization," 2016.
- [70] N. Srivastava, G. Hinton, A. Krizhevsky, I. Sutskever, and R. Salakhutdinov, "Dropout: a simple way to prevent neural networks from overfitting," *The journal of machine learning research*, vol. 15, no. 1, pp. 1929–1958, 2014.
- [71] C. Wu, F. Wu, T. Qi, and Y. Huang, "NoisyTune: A little noise can help you finetune pretrained language models better," in *Proceedings of the 60th Annual Meeting of the Association for Computational Linguistics (Volume 2: Short Papers)*. Dublin, Ireland: Association for Computational Linguistics, May 2022, pp. 680–685.
- [72] Y. Xu, Y. Sun, Y. Li, Y. Shi, X. Zhu, and S. Du, "Mh-detr: Video moment and highlight detection with cross-modal transformer," 2023.
- [73] J. Carreira and A. Zisserman, "Quo vadis, action recognition? a new model and the kinetics dataset," in *proceedings of the IEEE Conference on Computer Vision and Pattern Recognition*, 2017, pp. 6299–6308.
- [74] X. Glorot and Y. Bengio, "Understanding the difficulty of training deep feedforward neural networks," in *Proceedings of the thirteenth international conference on artificial intelligence and statistics*, JMLR Workshop and Conference Proceedings. Sardinia, Italy: JMLR, 2010, pp. 249–256.
- [75] I. Loshchilov and F. Hutter, "Decoupled weight decay regularization," 2019.
- [76] B. Xiong, Y. Kalantidis, D. Ghadiyaram, and K. Grauman, "Less is more: Learning highlight detection from video duration," in *Proceedings of the IEEE/CVF conference on computer vision and pattern recognition*. Long Beach, CA, USA: IEEE/CVF, 2019, pp. 1258–1267.
- [77] L. Wang, D. Liu, R. Puri, and D. N. Metaxas, "Learning trailer moments in full-length movies with co-contrastive attention," in *Computer Vision—ECCV 2020: 16th European Conference, August 23–28, 2020, Proceedings, Part XVIII 16*, Springer. Glasgow, UK: Springer International Publishing, 2020, pp. 300–316.
- [78] M. Xu, H. Wang, B. Ni, R. Zhu, Z. Sun, and C. Wang, "Cross-category video highlight detection via set-based learning," in *Proceedings of the IEEE/CVF International Conference on Computer Vision*. Virtual: IEEE/CVF, 2021, pp. 7970–7979.